HHS Public Access

Author manuscript

Curr Top Med Chem. Author manuscript; available in PMC 2016 January 01.

Published in final edited form as:

Curr Top Med Chem. 2015 ; 15(12): 1138–1152.

Applications of Aptamers in Targeted Imaging: State of the Art

Casey A. Dougherty[1], **Weibo Cai**[2,3,4,*], and **Hao Hong**[1,*]

[1]Department of Radiology, University of Michigan - Ann Arbor, Michigan 48109-2200, United States

[2]Department of Radiology, University of Wisconsin - Madison, Wisconsin 53705-2275, United States

[3]Department of Medical Physics, University of Wisconsin - Madison, Wisconsin 53705-2275, United States

[4]University of Wisconsin Carbone Cancer Center, Madison, Wisconsin 53705-2275, United States

Abstract

Aptamers are single-stranded oligonucleotides with high affinity and specificity to the target molecules or cells, thus they can serve as an important category of molecular targeting ligand. Since their discove1y, aptamers have been rapidly translated into clinical practice. The strong target affinity/selectivity, cost-effectivity, chemical versatility and safety of aptamers are superior to traditional peptides- or proteins-based ligands which make them unique choices for molecular imaging. Therefore, aptamers are considered to be extremely useful to guide various imaging contrast agents to the target tissues or cells for optical, magnetic resonance, nuclear, computed tomography, ultra sound and multimodality imaging. This review aims to provide an overview of aptamers' advantages as targeting ligands and their application in targeted imaging. Further research in synthesis of new types of aptamers and their conjugation with new categories of contrast agents is required to develop clinically translatable aptamer-based imaging agents which will eventually result in improved patient care.

Keywords

Aptamer; molecular imaging; nanomaterials; SELEX

1.INTRODUCTION

By a strict definition, aptamers are single-stranded (ss) DNA or RNA molecules (usually in a length of 20 - 100 bases) that possess strong and specific binding capacities to given

*Address correspondence to these authors at the Department of Radiology, University of Wisconsin - Madison, Wisconsin 53705-2275,United States; Tel: 1-608-262-1749; Fax: 1-608-265-0614; wcai@uwhealth.org and Department of Radiology,University of Michigan - Ann Arbor, Michigan 48109-2200, United States; Tel: 1-734-615-4634;Fax: 1-734-615-1599; hahong@med.umich.edu.

CONFLICT OF INTEREST

The authors confirm that this article content has no conflict of interest.

targets (organic/inorganic molecules, peptides, proteins, or live cells) [1]. Since their debut in the early 1990s [2, 3], aptamers have been widely used for treatment of various diseases. The core values of an aptamer lie in the fact that it can provide unique three-dimensional (3-D) structure via self-folding, which enables it to form stable complexes with theoretically any target molecule [4]. Serving as escort molecules, aptamers can be applicable in drug delive1y [5], cell targeting [6], proteomics [7], and targeted imaging [8]. In addition to oligonucleotides-based aptamers, another category of so-called peptide aptamers (combinatorial protein molecules) with unique structures could also perform similar functions [9]. The screening of peptide aptamers is distinct from oligonucleotide aptamers and will not be discussed in this review.

Aptamers are screened from random ssDNA or RNA library (containing up to 10^{16} DNA/RNA sequences) via a process called “systematic evolution of ligands by exponential enrichment (SELEX)” [10]. Conventional SELEX involves four steps (Scheme **1**): (1) synthesis of nucleic acid library composed of random sequences, (2) incubation with target molecule(s) for binding, (3) removal of unbound nucleic acids by washing and elution of bound nucleic acids, and (4) amplification of eluted DNA/RNA by polymerase chain reaction (PCR). This selection/amplification procedure undertaken by conventional SELEX is usually against purified protein targets. However, the use of purified protein is not ideal since most extracellular proteins in a physiological environment can be chemically/structurally modified (e.g. glycosylation) or masked by other factors so the binding profile with selected aptamers may be different. In certain cases, the target in a “natural” structure is potentially unrecognizable to screened aptamers [11]. To produce aptamers with higher targeting accuracy in a biological setting, cell-based SELEX has been developed, which targets live cells [12]. This strategy can ensure the interaction between aptamers and their targets in their nature conformations. One of the advantages of cell-based SELEX lies in the fact that it can generate aptamers for a certain cell line based on the individual extracellular characteristics without knowledge of its extracellular protein profiles [13]. However, potential non-specific interaction between DNA/RNA and lysine- or arginine-rich extracellular proteins inside cell-based SELEX cycles can result in compromised selectivity of produced aptamers, although this issue can be partially addressed by an increase of selection cycles [12].

During the last several decades, there has been remarkable progress in molecular imaging, which is an indispensable tool for both bench and bedside applications [14, 15]. Using an array of imaging techniques such as optical imaging (including fluorescence and bioluminescence), magnetic resonance imaging (MRI), positron emission tomography (PET), single photon emission computed tomography (SPECT), computed tomography (CT), ultrasound (US) etc., various dynamic biological processes can be monitored in intact living subjects. Molecular imaging is a unique asset to further our understanding of the underlying biology of various diseases, perform early disease detection and characterization, and assess the responses for a specific therapeutic intervention.

Regardless of the modality used, molecular imaging is generally achieved by accumulation of a probe into a target site and detection of the probe distribution. One of the conundrums in molecular imaging is to find a suitable probe which can possess good target-to-

background signals, high biocompatibility, low toxicity, and suitable stability [16]. Due to the affinity and specificity for their target(s), aptamers are sometimes referred as “chemical antibodies” [17]. Besides the observed high target affinity/specificity, aptamers are also economical, easy to synthesize or modify, comparatively stable, and capable of fast penetration into different tissues. In addition, unlike antibodies, they initiate minimal immune responses *in vivo*. Thus, it is envisaged that development of molecular imaging probes based on aptamers is a promising strategy to detect a wide range of diseases (Scheme **1**). Due to the focus of this review, we choose to elaborate on their applications in targeted imaging in living animals. The major imaging modalities used with aptamers have been outlined with discussions about pros/cons of each modality. Future directions of development are also predicted in this review.

2. FLUORESCENCE IMAGING WITH APTAMERS

Fluorescence is the most frequently adapted imaging tool in aptamer research due to its low cost and high sensitivity. It has been extensively used for aptamer-based protein recognition [18], cell separation/detection [19], or biomarker discovery [20]. Fluorescently labeled aptamers can be used as useful tools for highly sensitive cell imaging/detection. One good example is that an aptamer targeting mucin 1 (MUC-1) protein (overexpressed on the surface of many cancer cells [21]) -conjugated quantum dots (QD) could achieve a detection sensitivity of 100 MUC-1 positive cells per milliliter [22]. Another recent study adopted aptamers-conjugated barcode nanoparticles for detection of circulating tumor cells (CTC) in a reliable manner [23]. Interested readers can turn to a few comprehensive reviews to acquire further knowledge on aptamers’ applications in cell imaging/identification [10, 12, 17]. Despite the predominant usage of aptamers for cell-related applications, the case numbers of their applications in *in vivo* fluorescent imaging were quite limited. The following sections will categorize the aptamer-based fluorescent agents based on their imaging strategies and target selections - they will be primarily divided into two categories: direct labeling agents and low-background aptamer probes.

2.1. Directly Fluorescently Labeled Aptamer Probes

An aptamer needs to be chemically modified by a fluorophore (preferably with near-infrared (NIR) fluorescence emission for better tissue penetration [24]) before its application *in vivo.* Three types of targets prevailed in the fluorescence imaging applications with aptamers: live cells (with or without surface target identified), nucleolin, and MUC-1. Nucleolin is a protein located primarily in the nucleolus, but also found in the nucleoplasm, cytoplasm and cell membrane. Nucleolin's participation in disease (particularly cancer and viral infection) is associated with its ability to bind target RNAs via its four RNA-binding domains and its arginine/glycine rich domain [25]. Cell-swface nucleolin has been validated as a novel target for anticancer therapy. AS-1411 is the first and most popular aptamer for nucleolin targeting, which entered phase I/II clinical trials for the potential treatment of different types of cancer [26]. This guanine-rich aptamer has unmodified phosphodiester linkages and forms a G-quadruplex structure which leads to enhanced resistance to serum nuclease degradation and renders it particularly suitable for *in vivo* applications. In addition, as mentioned in the previous content, MUC-1 is a heterodimeric protein aberrantly

overexpressed in various types of cancers [27]. Inhibitors of the MUC-1 subunit have been developed that directly block its oncogenic function and induce cancer cell death in xenograft models. Aptamers against MUC-1 usually possess good specificity.

The initial report of aptamer-based fluorescence imaging was carried out in early 2010s to delineate tumor cells inside a mouse. A Cy5-labeled aptamer TD05 (Cy5-TD05, specific for Ramos, a B-cell lymphoma) was used as the imaging agent for *in vivo* fluorescence imaging in Ramos tumor-bearing nude mice [28]. After the intravenous injection, whole-body fluorescence imaging was used to determine the spatial and temporal distribution of Cy5-TD05. The results demonstrated that Cy5-TD05 could effectively recognize Ramos tumors with high sensitivity and selectivity, although potential degradation from nuclease was the major limitation of this study. With slight structural modification, TD05 aptamer was used in a recent study and attached onto QDs with polymeric surface for fluorescence imaging of cancer cells [29]. The aptamer-QD exhibited an enhanced fluorescence with recording time and was thus considered suitable for long-term cellular imaging.

Another aptamer-based fluorescence probe for carcinomas was identified via whole cell-based SELEX [30]. In this study, an aptamer (named S6) against A549 lung carcinoma cells, was labeled with Cy5. Flow cytometry assays confirmed that Cy5-S6 could specifically target A549 cells in both buffer and serum settings. *In vivo* fluorescence imaging also demonstrated the high specificity of Cy5-S6 for identification of A549 carcinoma (Fig. **1A**). After intravenous injection into nude mice simultaneously bearing A549 lung carcinoma and Tca8113 tongue carcinoma (off-target), a much longer retention time of Cy5-S6 in A549 tumor was observed. This strategy is universally applicable for carcinoma aptamer screening since two other aptamers (i.e. LS2 and ZY8, which were against Bel-7404 and SMMC-7721 liver carcinoma cells respectively) also showed effectivity in differentiating liver carcinomas of different subtypes in the same body.

Despite the structural advantages, the utilization of fluorescently labeled AS1411 in living animals as a nucleolin-targeting probe is still at a preliminary stage - the majority of them were only used for cell imaging to the best of our knowledge. In one study, *in situ* labeling and imaging of HeLa cancer cells was achieved by utilizing AS1411 conjugated with its fluorescent ligand, protoporphyrin IX (PPIX) [31]. A cellular confocal microscope assay confirmed that AS1411-PPIX complex was capable to distinguish nucleolin-overexpressed HeLa cells from normal cells in human serum.

Due to the facilitation of multivalent binding, AS1411 conjugated nanomaterials were frequently used as imaging agents. One AS1411-functionalized fluorescent gold nanoparticles (named NAANPs) is synthesized and successfully applied for both targeted cancer cell imaging and photodynamic therapy (PDT) [32]. The composition of NAANPs was AS1411 functionalized gold nanoparticles bound with fluorescent N-methylmesoporphyrin IX (NMM). The significantly increased fluorescence intensity of NMM upon binding to AS1411 G-quadruplex makes the NAANPs an appropriate fluorescence reagent for cell imaging. Meanwhile, NMM can also be used as a photosensitizer, thus irradiation of the NAANPs by the white light can lead to the production of reactive oxygen species for PDT. Gold nanoparticles here serve as both carrier and

enhancer of the functional groups onto the cells. The introduction of AS1411 onto water-soluble QDs was also carried out recently, which was synthesized in a microwave-assisted, one-stage manner [33]. AS1141-QDs showed efficient entrance into the nucleolin-positive U87MG glioblastoma cells.

MUC-1 aptamer-conjugated Rubpy-doped silica nanoparticles (SiNPs) were prepared in one study for MCF-7 cells (MUC-1 positive) labeling [34]. Probes prepared through direct covalent conjugation, biotin-avidin interaction, and a flexible polyethylene glycol (PEG) linker between the MUC-1 aptamer and carboxyl-modified Rubpy-doped SiNPs. The highest affinity for MUC-1 was observed on aptamer-SiNP with a PEG linker by fluorescence microscopy. In another study, MUC-1 aptamer and AS1411 conjugated magnetic beads and QD were used for selective collection and detection of MCF-7 [35]. Improved selectivity and detection sensitivity were obtained by simultaneous usage of these two aptamers as recognition elements, as compared with single aptamer. Drawn on the experiences from these studies, a MUC-1 aptamer was recently used for the *in vivo* tumor targeting, monitored by fluorescence imaging [36]. A NIR fluorescent dye (i.e. MPA) and PEG were conjugated to a MUC-1 aptamer. The PEG-modified probe exhibited better accumulation in MUC-1 positive cells (e.g. MCF-7) and slightly improved contrast for MUC-1 positive tumors *in vivo*. Parallel to this study, another MUC-1 aptamer was investigated in 3-D cell aggregates (multicellular spheroids of MCF-7 cells) and compared to an anti-MUC-1 antibody for its capacity to visualize cancer cells [37]. Results showed that MUC-1 antibodies interacted only with cells located on the surface of the spheroid, whereas the MUC-1 aptamers were able to penetrate inside these 3-D tumor models.

MUC-1 aptamer-conjugated QDs are another applicable probe for fluorescence imaging. Novel daunorubicin (DNR)-loaded MUC-1 aptamer QDs (DNR-MUC1-QDs) conjugates were formed for prostate cancer detection [38]. DNR was loaded by intercalating into the double-stranded CG sequence of the MUC-1 aptamers. DNR-MUC1-QDs can not only deliver DNR to the targeted cancer cells, but also can sense DNR release by the change of fluorescence from QDs. Another MUC-1 aptamer-QDs were developed through a facile one-pot hydrothermal method [39]. These MUC-1 aptamer-QDs have been successfully applied in active tumor-targeted imaging *in vitro* and *in vivo*. This efficient preparation method for MUC-1 aptamer-QDs could be easily adapted to other aptamer sequences.

Other targets that have been imaged or tracked by fluorescent aptamers include epithelial cell adhesion molecule (EpCAM) [40, 41], thrombin [42], or amyloid plaques [43]. EpCAM is overexpressed in most solid cancers and most of the EpCAM-based diagnostic, prognostic, and therapeutic strategies resort to the use of an anti-EpCAM antibody. Different DNA aptamers against human recombinant EpCAM were successfully identified in one study [40]. Among all aptamer sequences identified, a hairpin-structured sequence SYL3C was chosen due to a nanomolar dissociation constant (K_d). Flow cytometry analysis results indicated that the SYL3C aptamer was able to recognize target cancer cells from mixed cells in cell media. In another work, aptamer-conjugated carbon nanodots (C-Dots) have been employed as fluorescent probes for imaging/detection of thrombin [42]. The interaction with thrombin can induce the aptamer-modified fluorescent C-Dots to form a sandwich structure with aptamer-functionalized silica nanoparticles. An impressive detection limit of 1 nM for

thrombin is obtained in this study. More recently, a highly specific and sensitive optical imaging agent using aptamer for amyloid plaques was developed [43]. Fluorescently tagged anti-amyloid β RNA aptamer, β55, was found to bind amyloid plaques in both human Alzheimer's disease brain tissue and APP/PS1 transgenic mice.

As we stated in the previous text, cell-based SELEX is now intensively used for the selection of aptamers against cell surface biomarkers. However, despite negative selection steps using mock (negative-control) cells, this method sometimes results in aptamers against undesirable targets that are expressed both on mock and targeted cells. In an interesting study, the researchers suggested that it was possible to pull viable candidates from these "junk" aptamers for different applications from those originally envisaged [44]. Aptamers identification was originally performed against CHO-K1 cells expressing human Endothelin type B receptor (ETBR) using CHO-K1 cells as the control. No screened aptamers could however discriminate between both cell lines. One aptamer named ACE4 was later identified to bind selectively with the Annexin A2, a protein overexpressed in many cancers. After the cellular evaluation, tumor targeting using ACE4 was carried out *in vivo* in nude mice bearing MCF-7 xenografts. The aptamer demonstrated a significantly higher uptake in the tumor compared to a scramble sequence.

2.2. Low-Background Aptamer-Based Probes Via Energy Transfer

The imaging results from "always-on" fluorescent aptamer probes could be debatable in certain scenarios due to undesired background and limited contrast. To address this problem, different activatable aptamer-based probes (AAPs) were created for targeting membrane proteins of cancer cells and achieved contrast-enhanced cancer visualization inside the animals based on the mechanism of Förster resonance energy transfer (FRET). These AAPs usually displayed a quenched fluorescence in its free state and was able to undergo a conformational alteration upon binding to the target with an activated fluorescence. One good example for cellular application is a recently developed aptamer-conjugated polydiacetylene imaging probe that shows highly specific fluorescence switching upon binding to epithelial cancer cells that overexpress EpCAM on their surface [41]. Another interesting new study produced an activatable imaging probe by adoption of fluorescence-quenched complementary sequence for an aptamer, applicable as a turn-on agent for imaging of aptamers in bacteria [45].

One proof-of-concept study was conducted in CCRF-CEM cells (human acute lymphoblastic leukemia T cells which overexpress protein tyrosine kinase 7 (PTK7)) using AAPs based on an aptamer named sgc8 (targeting PTK7 [46]) [47]. It was confirmed that this sgc8-based AAP could be specifically activated by CCRF-CEM cells with fluorescence enhancement and exhibit a good detection sensitivity for CCRF-CEM cell (as low as 118 cells can be detectable). *In vivo* studies demonstrated that activated fluorescence signals were obviously achieved in the CCRF-CEM tumor sites in mice. Compared to always-on aptamer probes, the AAP could considerably minimize the background signal from non-target tissues, resulting in significantly enhanced image contrast and shortened diagnosis time.

Various nanoplatforms were frequently used for generation of AAPs. One example was self-assembly of a thiolated aptamer and a Cy5-labeled complementary DNA on the surface of Au@Ag/Au nanoparticles (NPs), which served as a quencher in this study [48]. The quenched fluorescence from this aptamer nanoplatform could be reactivated upon binding onto target and subsequent conformational change. By using S6 aptamer as the model, *in vitro* and *in vivo* studies of A549 lung cancer verified that this AAP greatly improved imaging contrast (Fig. **1B**). Another multifunctional nanomicelle was made for cancer targeting and therapy using a different AAP concept [49]. Instead of using a fluorescence quencher, the nanomicelle encapsulates a pH-activatable fluorescent probe and is functionalized with an aptamer. The fluorescent probe could light up the lysosomes for real-time imaging.

Another elegantly designed study employed an AS1411 aptamer and miRNA-221 molecular beacon (miR-221 MB)-conjugated magnetic fluorescence (MF) nanoparticle (MFAS miR-221 MB) as a cancer-targeting therangostics probe [50]. The goal of this study was to detect intracellular expression of miRNA-221 and treat miRNA-221-involved carcinogenesis. AS1411 here served as a targeting ligand which enabled MFAS nanoparticles to be selectively delivered into nucleolin-positive cancer cells. The miR-221 MB detached from the MFAS miR-221 MB in the cytoplasm of C6 cells could visualize the production of miRNA-221 and simultaneously resulted in antitumor therapeutic effects by inhibiting miRNA function. This MFAS miRNA MB technology can be easily applied to other cancers by simply changing a targeted miRNA. The previously mentioned TD05 aptamer was used in another study with the subtle utilization of the interactions between aptamer and nucleases - PEI/aptamer molecular complexes were generated for cancer imaging by using deoxyribonuclease (DNase)-activatable fluorescence to monitor DNA degradation [51]. The results showed that the complexes with PEI effectively protected TD05 aptamers from DNase degradation without affecting its affinity for Ramos cells. In tumor bearing mice, PEI/aptamer complexes further demonstrated superior passive tumor targeting and extended circulation time as compared with free TD05 aptamer. This well-defined PEI/aptamer probe can serve as a new tool to deliver targeted aptamer for tumor diagnosis and imaging *in vivo*.

The production of AAPs usually involves complex design and synthesis, and their stability in the biological system is not always satisfactory. To partially overcome these limitations, a novel strategy was proposed for cancer cell probing based on fluorophore-labeled aptamer/single-walled carbon nanotube (SWNT) ensembles [52]. Through π-stacking interactions and energy transfer, F-apt/SWNT with quenched fluorescence in its free state could produce signal activation upon the interaction with the target. Sgc8c aptamer was used in this study for *in vitro* analysis and *in vivo* imaging of CCRF-CEM. Cy5-Sgc8c/SWNT was robustly stable with ultralow background. When activated by target cells, Cy5-Sgc8c/SWNT could produce extremely high fluorescence elevation - the detection sensitivity could be as low as 12 CCRF-CEM cells out of 100 000 nontarget cells. The general applicability of the strategy was also confirmed by detecting Ramos cells with the TD05 aptamer. Similar strategies were also adopted in a nanographene oxide platform [53].

QD-aptamer-doxorubicin conjugate [QD-Apt(Dox)] was used as another low-background platform for cancer imaging, therapy, and sensing [54]. The aptamer used in this study is named A10 which recognizes the extracellular domain of the prostate specific membrane antigen (PSMA). Dox, a commonly used fluorescent antineoplastic drug, was introduced in the double-stranded stem of the A10 aptamer with reversible self-quenching properties. A donor-acceptor FRET between QD and Dox, and a donor-quencher FRET between Dox and A10 could both take place based on the interaction status between Dox and A10. This simple nanoplatform can deliver Dox to the targeted prostate cancer cells and sense the delivery of Dox by activating the fluorescence of QD, which concurrently images the cancer cells. Another aptamer-based FRET probes based on a peptide-thrombin binding aptamer conjugate was introduced together with streptavidin and biotinylated nuclear export signal peptide into HeLa cells, the resulting ternary complex enabled visualization of K^+ concentration changes in the cell [55]. A reporter system that consists of a FRET biosensor and its corresponding aptamer was described in another study [56]. The FRET biosensor employed a peptide Rsg1.2 inserted between mutants of fluorescent proteins, which could undergo FRET when interact with its aptamer.

3. MRI WITH APTAMERS

MRI allows the non-invasive visualization of internal structure and soft tissue morphology by usage of a powerful magnet and radiofrequency energy [57]. The basic principles of MRI are similar to those for nuclear magnetic resonance (NMR) and allow imaging of atomic nuclei within the body. The predominantly used nucleus for clinical MRI is ^1H in tissue water, from which most anatomical images are produced. One active area of MRI research is the development of novel MRI contrast agents that can produce a contrast in response to small molecules or biomarkers *in vivo*. To develop a general platform for obtaining MRI agents for any molecule of choice, aptamers are attractive choices due to the previously stated reasons after they are combined with a MRI label.

One category of aptamer-based MRI contrast agents or probes are based on the relaxation time change caused by conformational alteration of aptamers during the interactions with their targets. Similar to those used in fluorescence imaging, the concept of “activatable” probes is repeatedly used here. An early study was carried out to produce a “turn-on” MRI agent using superparamagnetic iron oxide nanoparticles (SPIOs) functionalized by aptamers [58] - the conjugation of adenosine-targeted aptamers was efficient to dephase the spins of neighboring water protons, leading to alteration in the spin-spin relaxation time (T2). The presence of increase concentration adenosine caused the release of the aptamers from SPIOs, resulting in dissociation of clustered SPIOs and brightness enhancement in a T2-weighted MR image. Similar “aptamer detaching” strategy was adopted by the same group for sensing of adenosine based on aptamer-streptavidin-gadolinium complex [59]. *In vivo* MR imaging was not conducted in either of these studies, but this design concept may be useful for future *in vivo* detection of various targets. In another proof-of-concept study, a thrombin aptamer was conjugated to diethylenetriaminepentaacetic (DTPA) dianhydride to form a monoamide derivative of the linear open-chain chelate commonly used in contrast agent Magnevist® [60]. Relaxitivity enhancements were observed in the presence of thrombin compared to a control protein. It was also found by the researchers that the introduction of spacers between

the aptamer and the DTPA (to eliminate possible steric effects) did not improve the relaxation enhancement achieved in comparison to the original aptamer conjugate.

On the other hand, another category of aptamer-based MRI agents embraced the concept of aggregation or assembly of aptamers functionalized nanoparticles upon the interactions with target proteins or cells. The best example is a MRI contrast agent based on aptamer-conjugated SPIOs for the detection of thrombin [61]. The aptamer functionalized nanoparticles were able to form an assembly and enhance the MR signal in the presence of thrombin. A detectable change in MRI signal is observed with 25 nM thrombin in human serum, which was not observed with control proteins. In a recent study, one aptamer targeting activated endothelial cells was used for MRI detection of atherosclerosis plaque since the initiation of atherosclerosis is upon the dysfunction of endothelial cells [62]. Although only cellular MRI was conducted to validate its specificity, this aptamer can be used for detecting early stage atherosclerotic plaques. Subsequently, the biodistribution and toxicity of AS1411-conjugated Mn_3O_4@SiO_2 core-shell nanoprobes (NPs) were evaluated in human cervical carcinoma tumor-bearing mice by a T1 MRI [63]. The NPs were prepared by encapsulating a hydrophobic Mn_3O_4 core within a silica shell. Rhodamine was doped into the silica shell and the amphiphilic PEG was modified on the surface of the shell to improve its biocompatibility, before AS1411 was conjugated onto the end of the PEG chains as targeting ligands. By means of *in vitro* fluorescence confocal imaging and *in vivo* MRI, the AS1411-conjugated NPs have been demonstrated to have an effective targeting for nucleolin-positive tumors.

Besides the applications in diseases/biomarkers detection, aptamer-based MRI probes can be useful tools to elucidate the biology events (e.g. angiogenesis, gene regulation etc.). Angiogenesis, a multistep process regulated by various angiogenic factors, has a pivotal role in the initiation and progression of different diseases particularly cancer [64]. An understanding of angiogenesis in cancer is acutely required for effective cancer therapy. Among all the angiogenic factors, integrin $\alpha_v\beta_3$ is closely associated with cell migration and invasion during angiogenesis. Aptamer$_{\alpha v\beta 3}$ -conjugated magnetic nanoparticles (Apt$_{\alpha v\beta 3}$ -MNPs) were developed to enable precise detection of tumor vasculature by MRI [65]. Apt$_{\alpha v\beta 3}$ -MNPs exhibited good biocompatibility and efficient integrin targeting ability both *in vitro* and *in vivo* (Fig. **2A**). Another target-of-interest is vascular growth factor receptor 2 (VEGFR2) overexpressed on tumor vasculatures. An imaging nanoprobe based on hybridization of a magnetic nanocrystal with an aptamer for VEGFR2 was used for the detection of glioblastoma vasculature via MRI [66]. The aptamer-conjugated magnetic nanocrystal effectively targeted VEGFR2 in an orthotopic glioblastoma mouse model with no observable cytotoxicity.

The transcription factor (TF) network is crucial for regulation of gene expressions [67], however inadequate information has been collected for understanding the specific roles of these TFs. An aptamers against the binding sequence of TF AP-1 (named 5ECdsAP1) was used in one study to elucidate its mechanism of action in living brains after conjugation with SPIOs [68]. MRI with 5ECdsAP1-SPIO revealed that neuronal AP-1 TF protein levels were elevated in neurons of live male C57B6 mice after amphetamine (AMPH) exposure, and this elevation can be suppressed by treatment with SCH23390, a dopaminergic receptor

antagonist (Fig. **2B**). Specific binding between the 5ECdsAP1 aptamer and endogenous AP-1 protein was confirmed in this study. These data suggested the potential role of aptamers for protein-guided imaging and monitoring of gene transcription regulation.

In some cases, aptamer-conjugated nanoparticles can be used as both MRI agents and therapeutic agents simultaneously. The PSMA-targeted A10 aptamer was conjugated with SPIO to serve as both prostate cancer-specific MRI contrast agents and a drug loading/delivery platform [69]. A10-SPIO showed selective accumulation and enhanced drug delivery efficacy in the LNCaP ($PSMA^+$) xenograft mouse model. Another study adopted a multifunctional porous hollow magnetite nanoparticle (PHMNP) for targeted chemotherapy and MRI of cancer cells [70]. PHMNP was connected to the sgc8 aptamer via a heterobifunctional PEG linker. Multiple aptamers on the surface of one single PHMNP led to enhanced binding and uptake to target cancer cells due to the multivalent effect. Upon reaching the lysosomes of target cancer cells, the relatively low lysosomal pH level resulted in corrosion of the PHMNP pores, facilitating the release of doxorubicin to kill the target cancer cells. Another epirubicin-5TR1 aptamer (against MUC-1)-SPIO tertiary complex (Epi-5TR1-SPIO) was evaluated for the imaging and treatment of murine C26 colon carcinoma (MUC-1 positive) [71]. Cytotoxicity of Epi-5TR1-SPIO was lower in CHO-K1 cells (off-target) when compared to Epi alone. MRI indicated a high level of accumulation of SPIO within the tumor site. This complex could efficiently detect tumors when analyzed by MRI and inhibit tumor growth *in vivo*. Another study used a similar concept to develop a magnetic nanoparticle-aptamer probe and drug carrier for hepatocellular carcinoma treatment [72].

4. PET/SPECT IMAGING WITH APTAMERS

Nuclear imaging (including PET and SPECT) can monitor the biological events deep in the body and provide longitudinal assessment of the same patient with high detection sensitivity. The development of SPECT and PET imaging modalities, combined with the synthesis of radioactive molecules with increased specificity for different biological targets, promoted the field of nuclear medicine into a new era. Aptamers selected from SELEX have showed high sensitivity and specificity required for nuclear imaging probes

4.1. SPECT Imaging

SPECT imaging relies on the detection of γ-ray emissions from the radioisotopes by a gamma camera. The most common isotopes for SPECT imaging include ^{99m}Tc ($t_{1/2}$: 6 h), ^{111}In ($t_{1/2}$: 2.8 d), and radioactive iodine (^{123}I ($t_{1/2}$: 13.2 h), ^{131}I ($t_{1/2}$: 8.0 d)).

SPECT imaging with radiolabeled aptamers or aptamer conjugates is an underexplored research area despite the fact that the first report of aptamer-based SPECT agent can be traced back to late 1990s [73]. In this study, an aptamer inhibitor for neutrophil elastase was isolated with selective binding to activated neutrophils. After the radiolabeling with ^{99m}Tc, this aptamer was used for detection of inflammation in a rat model. The aptamer demonstrated preferential binding to activated neutrophil *in vitro* and higher target-to-background (T/B) ratio when compared with radiolabeled IgG, while its absolute uptake in inflammatory site was not optimal. Almost a decade later, another aptamer for tenascin-C,

named TTA1, was radiolabeled with ^{99m}Tc and used for imaging studies in glioblastoma (U251) and breast cancer (MDA-MB-435) tumor xenografts [74]. ^{99m}Tc-labeled TTA1 displayed rapid blood clearance from both renal and hepatic pathways, and fast but durable tumor penetration (a tumor-to-blood ratio of 50 achieved at 3 h p.i.). The tumor uptake of ^{99m}Tc-labeled TTA1 is dependent on the abundance of tenascin-C within the tumor. The impact of aptamer dose on tumor uptake was also investigated in this study, and the conclusion is that dose increase caused elevated radioactivity of aptamer in blood, which resulted in increased tumor accumulation. Although the detailed mechanisms remained to be elucidated, usage of nonbinding oligonucleotide for boosting early blood levels and tumor uptake may be considered a potential clinical strategy.

Subsequently, a series of aptamers against MUC-1 were selected and conjugated with ^{99m}Tc via novel cyclen-based ligands [75]. Multi-aptamer (tetrameric) complexes on a central chelating ligand were also generated with increased circulation retention and almost intact tumor penetration capacities. Unfortunately the ligands exhibited inefficient complexation with technetium which produced significant amount of non-specific organ uptake (e.g. large amount of radioactivity was observed in stomach). Additional optimization was attempted by the same group by using mercaptoace-tyldiglycine $(MAG)_2$ conjugation onto MUC-1 aptamers, and the biodistribution of ^{99m}Tc-labeled MAG_2-MUC1 aptamers was analyzed in mice bearing MCF-7 tumors [76]. Despite the fact that convenient and high-yield labeling of ^{99m}Tc was witnessed, the radiolabeled aptamers did not produce satisfactory T/B ratio in this study. Further development will be required before these aptamers can be used in a diagnostic scenario.

To enhance the performance of radiolabeled aptamers, different methods have been carried out. One way to circumvent their short circulation half-life and rapid kidney clearance is to increase their overall molecular weights by conjugation to PEG or nanomaterials. A more recent study adopted SPECT/CT to compare the targeting efficacy of aptamer- or antibody-conjugated hollow gold nanospheres (HAuNS) for epidermal growth factor receptor (EGFR) *in vivo* with the usage of ^{111}In labeling [77]. The persistent accumulation of EGFR aptamer-conjugated HAuNS (Apt-HAuNS) in EGFR-positive OSC-19 tumors is faster and higher than that of EGFR antibody-conjugated HAuNS (C255-HAuNS, Fig. **3A**). This finding, combined with cell binding evaluation and biodistribution studies, supported that EGFR aptamer is a more advantageous for tumor homing applications over EGFR antibody. Although additional studies are needed to validate the universality in other nanomaterials and clarify the mechanisms behind, this highly selective aptamer can be a promising candidate for image-guided drug delivery via nanomaterials or selective thermal ablation of EGFR-positive tumors.

4.2. PET Imaging

When compared with SPECT, PET can provide higher sensitivity [57] - it takes advantage of the unique γ-ray emissions from the decay of a positron. The ring detector of PET can monitor the annihilation events (i.e. two γ-photons with energy of 511keV and travelling at opposite directions) and convert the signals into sonograms, which will eventually be

reconstructed to produce tomographic images [78]. With increased availability, the current state-of-the-art small animal PET scanner can provide improved spatial resolution (~1 mm).

Although the benefits of aptamer for PET imaging were foreseeable [79], it took a long time before the first report of using PET isotope with aptamers was performed in 2011 [80]. ^{64}Cu ($t_{1/2}$ = 12.7 h) was used as a radiolabel and the impact of different chelators onto the binding specificity of the aptamer (named A10-3.2, against PSMA) was evaluated. Although the key parameters (e.g. temperature, pH, and reaction ratio etc.) for optimal radiolabeling of ^{64}Cu were established and the stability/binding affinities of aptamer conjugates was investigated, no actual PET imaging was conducted in this study. Similar strategy was used by another research group to clarify the *in vivo* kinetics of ^{64}Cu-labeled AS1411, in lung cancer [81]. Four chelators including DOTA, CB-TE2A, DOTA-Bn, and NOTA-Bn were used for ^{64}Cu labeling with the successful generation of high yields and specific activities. PET imaging in H460 tumor-bearing mice revealed that ^{64}Cu-CB-TE2A-AS1411 showed faster clearance, higher tumor uptake, and higher T/B ratio compared with ^{64}Cu-DOTA-AS1411 despite the fact that they both showed good stability and binding affinity for nucleolin *in vitro*. However, the target specificity of ^{64}Cu-CB-TE2A-AS1411 was not fully confirmed *in vivo* due to the lack of scrambled analogue of AS1411 with decreased activity against the target due to the high abundance of guanines in the sequence [82].

Aptamer-modified nanomaterials are also readily applicable for PET imaging. Recently, an AS1411 derivative with high affinity for nucleolin was used as a functionalization group to modify silica nanoparticles for PET/fluorescence imaging of tumor metastasis in lymph nodes [83]. Silica nanoconjugates with sizes of 200 nm or 20 nm (denoted as NC200 and NC20) were used in this study. NC20-AS1411 efficiently delineated the 4T1 metastasis in the lymph node (Fig. **3B**) with enhanced retention compared to NC20 without AS1411 conjugation (NC20-ctrl).

5. CT IMAGING WITH APTAMER-BASED PROBES

Similar to MRI, CT imaging is most commonly used to examine anatomical structures. Images are generated from the differential absorption of the X-rays by the various tissues with achievable resolution being ~ 50 μm. Iodinated contrast agents are often used to enhance contrast achievable between different soft tissues. CT has comparatively limited potential as a molecular imaging tool since designing contrast agents/probes for this modality is rather difficult. Nonetheless, gold nanoparticles (GNPs) have emerged as some of the most extensively utilized nanoplatforms for CT imaging and photothermal therapy [84].

Aptamer-conjugated GNPs were developed and used as a CT contrast agent for prostate cancer cells [85]. The surface of these GNPs were modified with the A10 aptamer by a two-step conjugation strategy which utilized the interactions between aptamer and its complementary repeating oligonucleotide. This strategy maintained the affinity of aptamer to its target while enabled efficient anti-cancer drug loading (doxorubicin was used as a model drug in this study). Silver staining (which visualized the location of A10-GNPs) and CT imaging of prostate cancer cell aggregates confirmed that A10-GNPs can selectively

accumulate in PSMA-positive LNCaP cells while have minimal absorption onto PSMA-negative PC-3 cells (Fig. **4**). The A10-GNPs developed in this study are more applicable as a drug delivery nanoplatform rather than an imaging contrast agent. Due to the inherently low sensitivity of CT imaging, no *in vivo* imaging was carried out in this study.

6. ULTRASOUND IMAGING WITH APTAMER-BASED PROBES

US is among the most frequently used imaging modalities in clinics due to its safety, low cost, good portability, good temporal resolution, and wide availability [86]. It detects the signals coming from interactions between high-frequency sound waves (usually between 1 and 20 MHz) and surrounding tissues when they travel inside the body. Another unique character of US lies in that it can serve as both an imaging method and a therapeutic tool - a technology named focused ultrasound mediated drug delivery has been confirmed by a number of studies to enhance delivery of therapeutic agents into traditionally inaccessible disease sites (e.g. brain tumors) [87]. Ultrasound contrast agents (which are typically acoustically active particles, e.g. micro- or nano-bubbles) have been used for investigation of different pathological processes including inflammation, thrombus, tumors, and neovascularization [88]. The sizes of these gasfilled US contrast agents range from to a few hundred nanometers to several micrometers.

In one study, the sgc8c aptamer was conjugated onto the nanobubbles via thiol-maleimide coupling [89]. The resulting nanobubbles demonstrated enhanced uptake into CCRF-CEM, validated by both flow cytometry and cellular US imaging. Since nano-size gas bubbles usually possess lower stability and shorter circulation time [88], no *in vivo* imaging was carried out in this study. The same research group thus furthered their study and used similar conjugation strategy to generate another sgc8c-conjugated lipid nanobubbles (named acoustic droplets in this study) [90]. The anti-cancer drug (i.e. doxorubicin) loaded acoustic droplets with the average size of ~480 nm could selectively accumulate onto CCRF-CEM cells (confirmed by cellular US imaging). In addition, enhanced cancer cell killing was witnessed via both mechanical cell destruction and elevated local drug release when a high-intensity focused ultrasound (HIFU) was applied. Despite the success of these two studies, it is generally accepted that nanobubbles are less echogenic than larger bubbles, thus aptamer-conjugated microbubbles are considered more preferred choices for targeted US imaging.

An early study in 2010 adopted computational modeling approach to optimize the target binding affinity and specificity of aptamer-conjugated microbubbles [91]. This model provided useful insights into the key parameters affecting micro-bubble target interaction including micro-bubble size, target density/type, shear rate etc. Surprisingly, aptamer-conjugated microbubbles demonstrated stronger adhesion to the target when compared with the same microbubbles conjugated with the same density of antibody. This study may enable a flexible, prospective design and optimization of microbubbles to enhance the clinical translation of ultrasound-based molecular imaging.

A category of stimulus-responsive or “smart” aptamer-conjugated microbubbles were developed utilizing the sequence complementary nature of DNA and RNA. The acoustic emission from microbubbles is produced from their pressure-driven size/morphology

fluctuations, which is dependent on the mechanical properties of encapsulating shells [92]. One recent study reported the development of aptamer-crosslinked microbubbles that only showed ultrasound contrast activation at the presence of thrombin (associated with clot formation) [93]. The incorporation of a thrombin aptamer crosslinking strand (TACS, possessing nM affinity for thrombin) created a network of crosslinks around the entire bubble shell to stiffen the shell, and the acoustic properties of TACS-conjugated microbubbles can be significantly altered upon the interactions with thrombin (Fig. **5A**). Ultrasound imaging revealed that TACS-conjugated microbubbles can generate ultrasound signals only in response to thrombin in active blood clots (Fig. **5B**). This thrombin-sensitive contrast agent will provide high clinical values to determine the activity of a clot and initiate proper therapy accordingly. The same research group then further stabilized the TACS-conjugated microbubbles with PEG and used them in a rabbit deep venous thrombosis model for clot detection [94]. It was found in this follow-up study that these TACS microbubbles were able to detect active blood clots which were sufficiently small and invisible by traditional contrast agents (Fig. **5C**). This stimulus-responsive strategy provides low or no background signal which allows immediate target recognition and is thus particularly useful for detection of water-soluble markers. It may also find potential applications for cancer detection by recognizing other targets such as VEGF family. To date it is still unknown whether this approach can be used for targeting of cell surface receptor since a sufficient number of cross-linking aptamers on these microbubbles must interact with the target to destabilize the shell and trigger the acoustic signal change [92].

7. APTAMER-BASED PROBES FOR OTHER IMGING TECHNIQUES

Besides the abovementioned “mainstream” molecular imaging modalities, some other “unconventional” imaging techniques have also been used for research into aptamer functions, however no *in vivo* evaluation has been reported to date. In one study, aptamer-conjugated magnetic nanoparticles (MNPs) were used with aptamer against tenascin-C (named GB-10) as the targeting ligand for glioblastoma targeting [95]. Transmission electron microscopy (TEM) and energy dispersive x-ray spectroscopy (EDS) were used as the imaging tools to monitor the interaction between GB-10 conjugated MNPs (the authors named them “nanosurgeons”) and glioblastoma cells. Enhanced cell death caused by hypothermia was confirmed when both GB-10-MNPs and rotational magnetic field were applied. Another imaging technique called second harmonic generation (SHG) imaging, which uses near infrared laser light to improving penetration depths, was used in another study with aptamer-functionalized gold nanocage assemblies [96]. A9 aptamer conjugated gold nanocage assemblies can be used for targeted SHG imaging of the LNCaP prostate cancer cell line. This SHG imaging probe was highly selective and able to distinguish targeted cancer cell lines from other nontargeted cell types.

8. MULTIMODALITY IMAGING WITH APTAMER-BASED PROBES

Among all molecular imaging techniques, no single modality can obtain sufficient information for a particular medical question [24]. For example, it is difficult to accurately quantify fluorescence signal in living subjects, particularly in deep tissues; MRI has high resolution yet it suffers from low sensitivity; nuclear imaging techniques have very high

sensitivity but possess relatively poor spatial resolution. A combination of various molecular imaging modalities can offer synergistic advantages. Aptamers have important roles in successful development of specific and multifunctional molecular imaging probes. An fluorescence/MR nanoprobe was fabricated based on PEG-coated gadolinium oxide (PEG-Gd_2O_3)/aptamer-Ag nanoclusters, for tracking cancer cells [97]. With this nanoprobe, MCF-7 tumor cells could be specifically tracked by both fluorescence imaging and magnetic resonance imaging *in vitro*. Another interesting nanoplatform was develop from aptamer-conjugated, gadolinium-doped luminescent and mesoporous strontium hydroxyapatite nanorods (Gd:SrHap nanorods) [98]. The high biocompatibility and biodegradability Gd:SrHap nanorods with blue fluorescence and paramagnetism could serve as a good contrast agent for dual fluorescence and MR imaging.

The concept of activatable aptamer-nanoplatform has been used in a very interesting recent study for fluorescence/MR imaging [99]. The structure was based on a redoxable manganese dioxide (MnO_2) nanosheets conjugated with PTK7-targeting sgc8 aptamer, fluorescence quencher, and intracellular glutathione (GSH)-activated MRI contrast agent. In the presence of target cells, the adsorption of aptamers on MnO_2 nanosheets could be weakened by aptamer-target interactions and resulted in fluorescence recovery, making it applicable for fluorescence imaging. After the endocytosis of MnO_2 nanosheets, the reduction by GSH could not only further increased the fluorescence signals but also produced concentrated Mn^{2+} for MRI application. Although *in vivo* imaging was also not carried out in this study, it provided a good prototype for future applications.

A multimodal nanoprobe named “simultaneously multiple aptamers and RGD targeting” (SMART) was developed in order to establish a platform with enhanced specificity and sensitivity for cancer detection [100]. Fluorescence, PET, and MRI analysis demonstrated that the SMART probe simultaneously targeting the nucleolin, integrin $\alpha_v\beta_3$ and tenascin-C had dramatically enhanced specificity and cancer accumulation in a wide range of cancer models when compared with cancer probes targeting a single cancer biomarker. The results demonstrated that the SMART cancer probe will be useful for the diagnosis of different cancers as a cancer master probe. Another multimodal cancer-targeted imaging system capable of concurrent fluorescence imaging, nuclear imaging, and MRI was developed [101]. A cobalt-ferrite nanoparticle surrounded by fluorescent rhodamine (designated MF) within a silica shell matrix was synthesized with the AS1411 (MF-AS1411). MF-AS1411 was further labeled with ^{67}Ga (MFR-AS1411). MFR-AS1411 nanoparticle showed specific fluorescence signals in nucleolinpositive C6 cells. The rhodamine fluorescence intensity and ^{67}Ga activity of MFR-AS1411 in tumor were enhanced in a dose-dependent manner. T2-weighted MR images of the same mice injected with MFR-AS1411 showed darker T2 signals inside the tumor region, compared with the MRI signal of the tumor region injected with MFR conjugated with scrambled RNA sequences.

9. CONSIDERATIONS AND FUTURE PERSPECTIVES FOR APTAMER-BASED PROBES

Aptamers are a relatively new class of targeting ligand and a good amount of research and clinical efforts are focused on adopting aptamers as therapeutic or diagnostic agents. The

first aptamer based therapeutic (named pegaptanib) was approved in 2004 for the treatment of age-related macular degeneration and several other aptamers are currently being evaluated in clinical trials [102]. With the spontaneous folding into well-defined 3-D structures, aptamers can produce high binding affinity, sensitivity, and specificity needed for *in vivo* molecular imaging inside living animals. In addition, their small sizes, low synthesis cost, easy largescale production, and chemical versatility further render them more attractive for imaging purposes [1]. The equilibrium dissociation constants of aptamers are usually in the picomolar to micromolar range (similar to that of antibodies) [103], which enables them to be used for various medical/biological applications.

Stringent specificity of aptamer is required to ensure accurate discrimination of target from the abundant molecule pools in a living subject. Although aptamers have successfully targeted a number of cell membrane proteins and cell lines, it remains difficult to develop high-affinity aptamers for certain proteins using the standard RNA and DNA. A method was proposed with the goal of developing aptamers for any protein to form a new class of aptamers termed “slow off-rate modified aptamer” (SOMAmer) [104]. The major advantage of this technique lies in the introduction of protein-like elements (e.g. functional groups that mimic amino acid side chains) to enhance chemical diversity. In addition, the conventional SELEX involves a number of time-consuming steps which reduce the efficiency and efficacy of aptamer selection. Optimization such as stimulus-response cell SELEX (utilizing asymmetric PCR) was adopted which enables aptamer selection to distinguish activated cells or “diseased” cells and greatly reduces time and cost [62].

Over the past two decades, we have witnessed an explosive expansion in research efforts for aptamer-based therapeutic/diagnostic agents, however the aptamers have been surprisingly understudied as imaging agents [105]. One major hindrance is their susceptibility to nuclease (DNase or RNase) degradation *in vivo*. This limitation can be partially overcome by conjugation of aptamers with nanomaterials or protecting chemicals such as PEI or PEG - this conjugation usually has little effect on the affinities of aptamers but it can dramatically increase the circulation half-life and *in vivo* stability of aptamers, thus enhancing *in vivo* aptamer activity. Another strategy is the adoption of chemical modifications to introduce nuclease resistance. Chemical modifications can be introduced to different parts of aptamers including the nucleosides, the phosphodiester backbone and the 5′ and 3′-termini [106-108].

From an imaging point of view, using aptamer in combination imaging modality, i.e. multimodality imaging should be the future trend. Strategies that combine nuclear imaging (very sensitive and highly quantitative) and non-radionuclide based approaches, e.g. optical imaging which can significantly facilitate *ex vivo* validation of the *in vivo* data and/or MRI which can provide anatomical information with high resolution are of particular interest. One clinical scenario where a PET/optical agent is particularly useful is that an initial PET scan is used to identify the location of tumor(s), and the fluorescent label can subsequently provide surgical guidance for the tumor position during a resection procedure. In addition, another important direction for aptamer-based imaging probes is the design of AAPs - the conformational “switch” triggered when aptamers bind to their targets can bring more advantageous signal-to-background ratio (usually several times higher, Fig. **2**) compared with those “always on” probes, which can bring a lower limit of detection for a given target.

Future efforts can be devoted to produce AAPs with improved stability, simplified synthesis method, and more delicate response rate for the given targets. In addition, with the development of new imaging labels and more improved nanoplatforms, aptamer-based probes should be an indispensable component for molecular imaging applications.

Besides the imaging agents described in this review, aptamers can also be used to deliver other anti-cancer agents such as therapeutic radioisotopes (e.g. α-particle emitters, β-particle emitters, and Auger electron emitters). For example, ^{225}Ac was used in a recent study to label a PSMA aptamer modified liposome for effective targeted therapy [109]. Despite all the progress, some issues remain to be investigated for aptamer as an imaging agent. In most of the studies, a target with high abundance was chosen (e.g. TTA-aptamer, for there were up to six binding sites per target for the aptamer). Studies for less abundant targets need to be pursued to validate the potency of these aptamers [110].

CONCLUSION

By SELEX screening, aptamers can be produced to bind any targets with high affinity and specificity via unique 3-D structures. Aptamers may be exploited for various biological/medical applications due to their simple synthesis methods, facile chemical conjugation with other molecules, and unique pharmacokinetics. Increased efforts have been put to develop clinically translatable aptamer-based agents for imaging applications, and since the proof-of-concept for active-targeted imaging has been well established, it has paved the way to personalized diagnosis.

ACKNOWLEDGEMENTS

This work is supported, in part, by the University of Michigan Department of Radiology, the National Institutes of Health (NIBIB/NCI 1R01CA169365 and P30CA014520), the Department of Defense (W81XWH-11-1-0644), and the American Cancer Society (125246-RSG-13-099-01-CCE).

REFERENCES

[1]. Banerjee J, Nilsen-Hamilton M. Aptamers: multifunctional molecules for biomedical research. J. Mol. Med. (Berl). 2013; 91:1333–42. [PubMed: 24045702]

[2]. Ellington AD, Szostak JW. *In vitro* selection of RNA molecules that bind specific ligands. Nature. 1990; 346:818–22. [PubMed: 1697402]

[3]. Tuerk C, Gold L. Systematic evolution of ligands by exponential enrichment: RNA ligands to bacteriophage T4 DNA polymerase. Science. 1990; 249:505–10. [PubMed: 2200121]

[4]. Zhu G, Ye M, Donovan MJ, Song E, Zhao Z, Tan W. Nucleic acid aptamers: an emerging frontier in cancer therapy. Chem. Commun. (Camb). 2012; 48:10472–80. [PubMed: 22951893]

[5]. Zhu J, Huang H, Dong S, Ge L, Zhang Y. Progress in aptamer-mediated drug delivery vehicles for cancer targeting and its implications in addressing chemotherapeutic challenges. Theranostics. 2014; 4:931–44. [PubMed: 25057317]

[6]. Lopez-Colon D, Jimenez E, You M, Gulbakan B, Tan W. Aptamers: turning the spotlight on cells. Wiley Interdiscip. Rev. Nanomed. Nanobiotechnol. 2011; 3:328–40. [PubMed: 21412992]

[7]. Thiviyanathan V, Gorenstein DG. Aptamers and the next generation of diagnostic reagents. Proteomics Clin. Appl. 2012; 6:563–73. [PubMed: 23090891]

[8]. Hong H, Goel S, Zhang Y, Cai W. Molecular imaging with nucleic acid aptamers. Curr. Med. Chem. 2011; 18:4195–205. [PubMed: 21838686]

[9]. Li J, Tan S, Chen X, Zhang CY, Zhang Y. Peptide aptamers with biological and therapeutic applications. Curr. Med. Chem. 2011; 18:4215–22. [PubMed: 21838684]

[10]. Mayer G. The chemical biology of aptamers. Angew. Chem. Int. Ed. Engl. 2009; 48:2672–89. [PubMed: 19319884]

[11]. Liu Y, Kuan CT, Mi J, Zhang X, Clary BM, Bigner DD, Sullenger BA. Aptamers selected against the unglycosylated EGFRvIII ectodomain and delivered intracellularly reduce membrane-bound EGFRvIII and induce apoptosis. Biol. Chem. 2009; 390:137–44. [PubMed: 19040357]

[12]. Tan W, Donovan MJ, Jiang J. Aptamers from cell-based selection for bioanalytical applications. Chem. Rev. 2013; 113:2842–62. [PubMed: 23509854]

[13]. Liu J, You M, Pu Y, Liu H, Ye M, Tan W. Recent developments in protein and cell-targeted aptamer selection and applications. Curr. Med. Chem. 2011; 18:4117–25. [PubMed: 21838693]

[14]. Weissleder R, Pittet MJ. Imaging in the era of molecular oncology. Nature. 2008; 452:580–9. [PubMed: 18385732]

[15]. James ML, Gambhir SS. A molecular imaging primer: modalities, imaging agents, and applications. Physiol. Rev. 2012; 92:897–965. [PubMed: 22535898]

[16]. Chakravarty R, Goel S, Cai W. Nanobody: the “magic bullet” for molecular imaging? Theranostics. 2014; 4:386–98. [PubMed: 24578722]

[17]. Syed MA, Pervaiz S. Advances in aptamers. Oligonucleotides. 2010; 20:215–24. [PubMed: 20677985]

[18]. Li JJ, Fang X, Tan W. Molecular aptamer beacons for realtime protein recognition. Biochem. Biophys. Res. Commun. 2002; 292:31–40. [PubMed: 11890667]

[19]. Pu Y, Zhu Z, Liu H, Zhang J, Liu J, Tan W. Using aptamers to visualize and capture cancer cells. Anal. Bioanal. Chem. 2010; 397:3225–33. [PubMed: 20480151]

[20]. Ulrich H, Wrenger C. Disease-specific biomarker discovery by aptamers. Cytometry A. 2009; 75:727–33. [PubMed: 19565638]

[21]. Ferreira CS, Matthews CS, Missailidis S. DNA aptamers that bind to MUC1 tumour marker: design and characterization of MUC1-binding single-stranded DNA aptamers. Tumour Biol. 2006; 27:289–301. [PubMed: 17033199]

[22]. Li J, Xu M, Huang H, Zhou J, Abdel-Halimb ES, Zhang JR, Zhu JJ. Aptamer-quantum dots conjugates-based ultrasensitive competitive electrochemical cytosensor for the detection of tumor cell. Talanta. 2011; 85:2113–20. [PubMed: 21872066]

[23]. Zheng F, Cheng Y, Wang J, Lu J, Zhang B, Zhao Y, Gu Z. Aptamer-functionalized barcode particles for the capture and detection of multiple types of circulating tumor cells. Adv. Mater. 2014; 26:7333–8. [PubMed: 25251012]

[24]. Massoud TF, Gambhir SS. Molecular imaging in living subjects: seeing fundamental biological processes in a new light. Genes Dev. 2003; 17:545–80. [PubMed: 12629038]

[25]. Abdelmohsen K, Gorospe M. RNA-binding protein nucleolin in disease. RNA Biol. 2012; 9:799–808. [PubMed: 22617883]

[26]. Mongelard F, Bouvet P. AS-1411, a guanosine-rich oligonucleotide aptamer targeting nucleolin for the potential treatment of cancer, including acute myeloid leukemia. Curr. Opin. Mol. Ther. 2010; 12:107–14. [PubMed: 20140822]

[27]. Kufe DW. MUC1-C oncoprotein as a target in breast cancer: activation of signaling pathways and therapeutic approaches. Oncogene. 2013; 32:1073–81. [PubMed: 22580612]

[28]. Shi H, Tang Z, Kim Y, Nie H, Huang YF, He X, Deng K, Wang K, Tan W. *In vivo* fluorescence imaging of tumors using molecular aptamers generated by cell-SELEX. Chem. Asian J. 2010; 5:2209–13. [PubMed: 20806314]

[29]. Jie G, Zhao Y, Qin Y. A fluorescent polymeric quantum dot/aptamer superstructure and its application for imaging of cancer cells. Chem. Asian J. 2014; 9:1261–4. [PubMed: 24616365]

[30]. Shi H, Cui W, He X, Guo Q, Wang K, Ye X, Tang J. Whole cell-SELEX aptamers for highly specific fluorescence molecular imaging of carcinomas *in vivo*. PLoS One. 2013; 8:e70476. [PubMed: 23950940]

[31]. Ai J, Li T, Li B, Xu Y, Li D, Liu Z, Wang E. In situ labeling and imaging of cellular protein via a bi-functional anticancer aptamer and its fluorescent ligand. Anal. Chim. Acta. 2012; 741:93–9. [PubMed: 22840709]

[32]. Ai J, Xu Y, Lou B, Li D, Wang E. Multifunctional AS1411-functionalized fluorescent gold nanoparticles for targeted cancer cell imaging and efficient photodynamic therapy. Talanta. 2014; 118:54–60. [PubMed: 24274270]

[33]. Alibolandi M, Abnous K, Ramezani M, Hosseinkhani H, Hadizadeh F. Synthesis of AS1411-aptamer-conjugated CdTe quantum dots with high fluorescence strength for probe labeling tumor cells. J. Fluoresc. 2014; 24:1519–29. [PubMed: 25172439]

[34]. Cai L, Chen ZZ, Chen MY, Tang HW, Pang DW. MUC-1 aptamer-conjugated dye-doped silica nanoparticles for MCF-7 cells detection. Biomaterials. 2013; 34:371–81. [PubMed: 23084552]

[35]. Hua X, Zhou Z, Yuan L, Liu S. Selective collection and detection of MCF-7 breast cancer cells using aptamer-functionalized magnetic beads and quantum dots based nano-bio-probes. Anal. Chim. Acta. 2013; 788:135–40. [PubMed: 23845492]

[36]. Chen H, Zhao J, Zhang M, Yang H, Ma Y, Gu Y. MUC1 aptamer-based near-infrared fluorescence probes for tumor imaging. Mol. Imaging Biol. Jul.2014 Epub.

[37]. Martinez O, Bellard E, Golzio M, Mechiche-Alami S, Rols MP, Teissie J, Ecochard V, Paquereau L. Direct validation of aptamers as powerful tools to image solid tumor. Nucleic Acid Ther. 2014; 24:217–25. [PubMed: 24490589]

[38]. Lin Z, Ma Q, Fei X, Zhang H, Su X. A novel aptamer functionalized $CuInS_2$ quantum dots probe for daunorubicin sensing and near infrared imaging of prostate cancer cells. Anal. Chim. Acta. 2014; 818:54–60. [PubMed: 24626403]

[39]. Zhang C, Ji X, Zhang Y, Zhou G, Ke X, Wang H, Tinnefeld P, He Z. One-pot synthesized aptamer-functionalized CdTe:Zn2+ quantum dots for tumor-targeted fluorescence imaging *in vitro* and *in vivo*. Anal. Chem. 2013; 85:5843–9. [PubMed: 23682757]

[40]. Song Y, Zhu Z, An Y, Zhang W, Zhang H, Liu D, Yu C, Duan W, Yang CJ. Selection of DNA aptamers against epithelial cell adhesion molecule for cancer cell imaging and circulating tumor cell capture. Anal. Chem. 2013; 85:4141–9. [PubMed: 23480100]

[41]. Jung YK, Woo MA, Soh HT, Park HG. Aptamer-based cell imaging reagents capable of fluorescence switching. Chem. Commun. (Camb). 2014; 50:12329–32. [PubMed: 25182171]

[42]. Xu B, Zhao C, Wei W, Ren J, Miyoshi D, Sugimoto N, Qu X. Aptamer carbon nanodot sandwich used for fluorescent detection of protein. Analyst. 2012; 137:5483–6. [PubMed: 23050264]

[43]. Farrar CT, William CM, Hudry E, Hashimoto T, Hyman BT. RNA aptamer probes as optical imaging agents for the detection of amyloid plaques. PLoS One. 2014; 9:e89901. [PubMed: 24587111]

[44]. Cibiel A, Quang NN, Gombert K, Theze B, Garofalakis A, Duconge F. From ugly duckling to swan: unexpected identification from cell-SELEX of an anti-Annexin A2 aptamer targeting tumors. PLoS One. 2014; 9:e87002. [PubMed: 24489826]

[45]. Sunbul M, Jaschke A. Contact-mediated quenching for RNA imaging in bacteria with a fluorophore-binding aptamer. Angew. Chem. Int. Ed. Engl. 2013; 52:13401–4. [PubMed: 24133044]

[46]. Shangguan D, Cao Z, Meng L, Mallikaratchy P, Sefah K, Wang H, Li Y, Tan W. Cell-specific aptamer probes for membrane protein elucidation in cancer cells. J. Proteome. Res. 2008; 7:2133–9. [PubMed: 18363322]

[47]. Shi H, He X, Wang K, Wu X, Ye X, Guo Q, Tan W, Qing Z, Yang X, Zhou B. Activatable aptamer probe for contrast-enhanced *in vivo* cancer imaging based on cell membrane protein-triggered conformation alteration. Proc. Natl. Acad. Sci. U S A. 2011; 108:3900–5. [PubMed: 21368158]

[48]. Shi H, Ye X, He X, Wang K, Cui W, He D, Li D, Jia X. Au@Ag/Au nanoparticles assembled with activatable aptamer probes as smart “nano-doctors” for image-guided cancer thermotherapy. Nanoscale. 2014; 6:8754–61. [PubMed: 24953128]

[49]. Tian J, Ding L, Ju H, Yang Y, Li X, Shen Z, Zhu Z, Yu JS, Yang CJ. A multifunctional nanomicelle for real-time targeted imaging and precise near-infrared cancer therapy. Angew. Chem. Int. Ed. Engl. 2014; 53:9544–9. [PubMed: 25045069]

[50]. Kim JK, Choi KJ, Lee M, Jo MH, Kim S. Molecular imaging of a cancer-targeting theragnostics probe using a nucleolin aptamerand microRNA-221 molecular beacon-conjugated nanoparticle. Biomaterials. 2012; 33:207–17. [PubMed: 21944470]

[51]. Gong P, Shi B, Zheng M, Wang B, Zhang P, Hu D, Gao D, Sheng Z, Zheng C, Ma Y, Cai L. PEI protected aptamer molecular probes for contrast-enhanced *in vivo* cancer imaging. Biomaterials. 2012; 33:7810–7. [PubMed: 22835645]

[52]. Yan L, Shi H, He X, Wang K, Tang J, Chen M, Ye X, Xu F, Lei Y. A versatile activatable fluorescence probing platform for cancer cells *in vitro* and *in vivo* based on self-assembled aptamer/carbon nanotube ensembles. Anal. Chem. 2014; 86:9271–7. [PubMed: 25153687]

[53]. Yi M, Yang S, Peng Z, Liu C, Li J, Zhong W, Yang R, Tan W. Two-photon graphene oxide/aptamer nanosensing conjugate for *in vitro* or *in vivo* molecular probing. Anal. Chem. 2014; 86:3548–54. [PubMed: 24592855]

[54]. Bagalkot V, Zhang L, Levy-Nissenbaum E, Jon S, Kantoff PW, Langer R, Farokhzad OC. Quantum dot-aptamer conjugates for synchronous cancer imaging, therapy, and sensing of drug delivery based on bi-fluorescence resonance energy transfer. Nano. Lett. 2007; 7:3065–70. [PubMed: 17854227]

[55]. Ohtsuka K, Sato S, Sato Y, Sota K, Ohzawa S, Matsuda T, Takemoto K, Takamune N, Juskowiak B, Nagai T, Takenaka S. Fluorescence imaging of potassium ions in living cells using a fluorescent probe based on a thrombin binding aptamer-peptide conjugate. Chem. Commun. (Camb). 2012; 48:4740–2. [PubMed: 22475983]

[56]. Schifferer M, Griesbeck O. A dynamic FRET reporter of gene expression improved by functional screening. J. Am. Chem. Soc. 2012; 134:15185–8. [PubMed: 22946509]

[57]. Gambhir SS. Molecular imaging of cancer with positron emission tomography. Nat. Rev. Cancer. 2002; 2:683–93. [PubMed: 12209157]

[58]. Yigit MV, Mazumdar D, Kim HK, Lee JH, Odintsov B, Lu Y. Smart “turn-on” magnetic resonance contrast agents based on aptamer-functionalized superparamagnetic iron oxide nanoparticles. Chembiochem. 2007; 8:1675–8. [PubMed: 17696177]

[59]. Xu W, Lu Y. A smart magnetic resonance imaging contrast agent responsive to adenosine based on a DNA aptamer-conjugated gadolinium complex. Chem. Commun. (Camb). 2011; 47:4998–5000. [PubMed: 21424019]

[60]. Bernard ED, Beking MA, Rajamanickam K, Tsai EC, Derosa MC. Target binding improves relaxivity in aptamer-gadolinium conjugates. J. Biol. Inorg. Chem. 2012; 17:1159–75. [PubMed: 22903502]

[61]. Yigit MV, Mazumdar D, Lu Y. MRI detection of thrombin with aptamer functionalized superparamagnetic iron oxide nanoparticles. Bioconjug. Chem. 2008; 19:412–7. [PubMed: 18173225]

[62]. Ji K, Lim WS, Li SF, Bhakoo K. A two-step stimulus-response cell-SELEX method to generate a DNA aptamer to recognize inflamed human aortic endothelial cells as a potential *in vivo* molecular probe for atherosclerosis plaque detection. Anal. Bioanal. Chem. 2013; 405:6853–61. [PubMed: 23842900]

[63]. Hu H, Dai A, Sun J, Li X, Gao F, Wu L, Fang Y, Yang H, An L, Wu H, Yang S. Aptamer-conjugated $Mn_3O_4@SiO_2$ core-shell nanoprobes for targeted magnetic resonance imaging. Nanoscale. 2013; 5:10447–54. [PubMed: 24057072]

[64]. Hong H, Chen F, Zhang Y, Cai W. New radiotracers for imaging of vascular targets in angiogenesis-related diseases. Adv. Drug Deliv. Rev. 2014; 76:2–20. [PubMed: 25086372]

[65]. Lim EK, Kim B, Choi Y, Ro Y, Cho EJ, Lee JH, Ryu SH, Suh JS, Haam S, Huh YM. Aptamer-conjugated magnetic nanoparticles enable efficient targeted detection of integrin $\alpha_v\beta_3$ via magnetic resonance imaging. J. Biomed. Mater. Res. A. 2013

[66]. Kim B, Yang J, Hwang M, Choi J, Kim HO, Jang E, Lee JH, Ryu SH, Suh JS, Huh YM, Haam S. Aptamer-modified magnetic nanoprobe for molecular MR imaging of VEGFR2 on angiogenic vasculature. Nanoscale Res. Lett. 2013; 8:399. [PubMed: 24066922]

[67]. Niwa H. The pluripotency transcription factor network at work in reprogramming. Curr. Opin. Genet. Dev. 2014; 28c:25–31. [PubMed: 25173150]

[68]. Liu CH, Ren J, Liu CM, Liu PK. Intracellular gene transcription factor protein-guided MRI by DNA aptamers *in vivo*. FASEB J. 2014; 28:464–73. [PubMed: 24115049]

[69]. Yu MK, Kim D, Lee IH, So JS, Jeong YY, Jon S. Image-guided prostate cancer therapy using aptamer-functionalized thermally cross-linked superparamagnetic iron oxide nanoparticles. Small. 2011; 7:2241–9. [PubMed: 21648076]

[70]. Chen T, Shukoor MI, Wang R, Zhao Z, Yuan Q, Bamrungsap S, Xiong X, Tan W. Smart multifunctional nanostructure for targeted cancer chemotherapy and magnetic resonance imaging. ACS Nano. 2011; 5:7866–73. [PubMed: 21888350]

[71]. Jalalian SH, Taghdisi SM, Shahidi Hamedani N, Kalat SA, Lavaee P, Zandkarimi M, Ghows N, Jaafari MR, Naghibi S, Danesh NM, Ramezani M, Abnous K. Epirubicin loaded super paramagnetic iron oxide nanoparticle-aptamer bioconjugate for combined colon cancer therapy and imaging *in vivo*. Eur. J. Pharm. Sci. 2013; 50:191–7. [PubMed: 23835028]

[72]. Pilapong C, Sitthichai S, Thongtem S, Thongtem T. Smart magnetic nanoparticle-aptamer probe for targeted imaging and treatment of hepatocellular carcinoma. Int. J. Pharm. 2014; 473:469–74. [PubMed: 25089503]

[73]. Charlton J, Sennello J, Smith D. *In vivo* imaging of inflammation using an aptamer inhibitor of human neutrophil elastase. Chem. Biol. 1997; 4:809–16. [PubMed: 9384527]

[74]. Hicke BJ, Stephens AW, Gould T, Chang YF, Lynott CK, Heil J, Borkowski S, Hilger CS, Cook G, Warren S, Schmidt PG. Tumor targeting by an aptamer. J. Nucl. Med. 2006; 47:668–78. [PubMed: 16595502]

[75]. Borbas KE, Ferreira CS, Perkins A, Bruce JI, Missailidis S. Design and synthesis of mono- and multimeric targeted radio-pharmaceuticals based on novel cyclen ligands coupled to anti-MUC1 aptamers for the diagnostic imaging and targeted radiotherapy of cancer. Bioconjug. Chem. 2007; 18:1205–12. [PubMed: 17583928]

[76]. Pieve CD, Perkins AC, Missailidis S. Anti-MUC1 aptamers: radiolabelling with ^{99m}Tc and biodistribution in MCF-7 tumour-bearing mice. Nucl. Med. Biol. 2009; 36:703–10. [PubMed: 19647177]

[77]. Melancon MP, Zhou M, Zhang R, Xiong C, Allen P, Wen X, Huang Q, Wallace M, Myers JN, Stafford RJ, Liang D, Ellington AD, Li C. Selective uptake and imaging of aptamer- and antibody-conjugated hollow nanospheres targeted to epidermal growth factor receptors overexpressed in head and neck cancer. ACS Nano. 2014; 8:4530–8. [PubMed: 24754567]

[78]. Chatziioannou AF. Instrumentation for molecular imaging in preclinical research: micro-PET and micro-SPECT. Proc. Am. Thorac. Soc. 2005; 2:533–6. 510-11. [PubMed: 16352760]

[79]. Lucignani G. Aptamers and in-beam PET for advanced diagnosis and therapy optimisation. Eur. J. Nucl. Med. Mol. Imaging. 2006; 33:1095–7. [PubMed: 16896657]

[80]. Rockey WM, Huang L, Kloepping KC, Baumhover NJ, Giangrande PH, Schultz MK. Synthesis and radiolabeling of chelator-RNA aptamer bioconjugates with copper-64 for targeted molecular imaging. Bioorg. Med. Chem. 2011; 19:4080–90. [PubMed: 21658962]

[81]. Li J, Zheng H, Bates PJ, Malik T, Li XF, Trent JO, Ng CK. Aptamer imaging with Cu-64 labeled AS1411: preliminary assessment in lung cancer. Nucl. Med. Biol. 2014; 41:179–85. [PubMed: 24373858]

[82]. Reyes-Reyes EM, Teng Y, Bates PJ. A new paradigm for aptamer therapeutic AS1411 action: uptake by macropinocytosis and its stimulation by a nucleolin-dependent mechanism. Cancer Res. 2010; 70:8617–29. [PubMed: 20861190]

[83]. Tang L, Yang X, Dobrucki LW, Chaudhury I, Yin Q, Yao C, Lezmi S, Helferich WG, Fan TM, Cheng J. Aptamer-functionalized, ultra-small, monodisperse silica nanoconjugates for targeted dual-modal imaging of lymph nodes with metastatic tumors. Angew. Chem. Int. Ed. Engl. 2012; 51:12721–6. [PubMed: 23136130]

[84]. Curry T, Kopelman R, Shilo M, Popovtzer R. Multifunctional theranostic gold nanoparticles for targeted CT imaging and photothermal therapy. Contrast Media Mol. Imaging. 2014; 9:53–61. [PubMed: 24470294]

[85]. Kim D, Jeong YY, Jon S. A drug-loaded aptamer-gold nanoparticle bioconjugate for combined CT imaging and therapy of prostate cancer. ACS Nano. 2010; 4:3689–96. [PubMed: 20550178]

[86]. Bloch SH, Dayton PA, Ferrara KW. Targeted imaging using ultrasound contrast agents. Progess and opportunities for clinical and research applications. IEEE Eng. Med. Biol. Mag. 2004; 23:18–29. [PubMed: 15565796]

[87]. Liu HL, Fan CH, Ting CY, Yeh CK. Combining micro-bubbles and ultrasound for drug delivery to brain tumors: current progress and overview. Theranostics. 2014; 4:432–44. [PubMed: 24578726]

[88]. Wen Q, Wan S, Liu Z, Xu S, Wang H, Yang B. Ultrasound contrast agents and ultrasound molecular imaging. J. Nanosci. Nanotechnol. 2014; 14:190–209. [PubMed: 24730259]

[89]. Wang CH, Huang YF, Yeh CK. Aptamer-conjugated nano-bubbles for targeted ultrasound molecular imaging. Langmuir. 2011; 27:6971–6. [PubMed: 21553884]

[90]. Wang CH, Kang ST, Lee YH, Luo YL, Huang YF, Yeh CK. Aptamer-conjugated and drug-loaded acoustic droplets for ultrasound theranosis. Biomaterials. 2012; 33:1939–47. [PubMed: 22142768]

[91]. Maul TM, Dudgeon DD, Beste MT, Hammer DA, Lazo JS, Villanueva FS, Wagner WR. Optimization of ultrasound contrast agents with computational models to improve selection of ligands and binding strength. Biotechnol. Bioeng. 2010; 107:854–64. [PubMed: 20665479]

[92]. Goodwin AP, Nakatsuka MA, Mattrey RF. Stimulus-responsive ultrasound contrast agents for clinical imaging: motivations, demonstrations, and future directions. Wiley Interdiscip. Rev. Nanomed. Nanobiotechnol. 2015; 7:111–123. [PubMed: 25195785]

[93]. Nakatsuka MA, Mattrey RF, Esener SC, Cha JN, Goodwin AP. Aptamer-crosslinked microbubbles: smart contrast agents for thrombin-activated ultrasound imaging. Adv. Mater. 2012; 24:6010–6. [PubMed: 22941789]

[94]. Nakatsuka MA, Barback CV, Fitch KR, Farwell AR, Esener SC, Mattrey RF, Cha JN, Goodwin AP. *In vivo* ultrasound visualization of non-occlusive blood clots with thrombin-sensitive contrast agents. Biomaterials. 2013; 34:9559–65. [PubMed: 24034499]

[95]. Nair BG, Nagaoka Y, Morimoto H, Yoshida Y, Maekawa T, Kumar DS. Aptamer conjugated magnetic nanoparticles as nanosurgeons. Nanotechnology. 2010; 21:455102. [PubMed: 20947949]

[96]. Demeritte T, Fan Z, Sinha SS, Duan J, Pachter R, Ray PC. Gold nanocage assemblies for selective second harmonic generation imaging of cancer cell. Chemistry. 2014; 20:1017–22. [PubMed: 24339156]

[97]. Li J, You J, Dai Y, Shi M, Han C, Xu K. Gadolinium oxide nanoparticles and aptamer-functionalized silver nanoclusters-based multimodal molecular imaging nanoprobe for optical/magnetic resonance cancer cell imaging. Anal. Chem. 2014; 86:11306–11. [PubMed: 25338209]

[98]. Li Z, Liu Z, Yin M, Yang X, Yuan Q, Ren J, Qu X. Aptamer-capped multifunctional mesoporous strontium hydroxyapatite nanovehicle for cancer-cell-responsive drug delivery and imaging. Biomacromolecules. 2012; 13:4257–63. [PubMed: 23140615]

[99]. Zhao Z, Fan H, Zhou G, Bai H, Liang H, Wang R, Zhang X, Tan W. Activatable fluorescence/MRI bimodal platform for tumor cell imaging via MnO_2 nanosheet-aptamer nanoprobe. J. Am. Chem. Soc. 2014; 136:11220–3. [PubMed: 25061849]

[100]. Ko HY, Choi KJ, Lee CH, Kim S. A multimodal nanoparticle-based cancer imaging probe simultaneously targeting nucleolin, integrin $\alpha_v\beta_3$ and tenascin-C proteins. Biomaterials. 2011; 32:1130–8. [PubMed: 21071077]

[101]. Hwang do W, Ko HY, Lee JH, Kang H, Ryu SH, Song IC, Lee DS, Kim S. A nucleolin-targeted multimodal nanoparticle imaging probe for tracking cancer cells using an aptamer. J. Nucl. Med. 2010; 51:98–105. [PubMed: 20008986]

[102]. Ni X, Castanares M, Mukherjee A, Lupold SE. Nucleic acid aptamers: clinical applications and promising new horizons. Curr. Med. Chem. 2011; 18:4206–14. [PubMed: 21838685]

[103]. Stoltenburg R, Reinemann C, Strehlitz B. SELEX--a (r)evolutionary method to generate high-affinity nucleic acid ligands. Biomol. Eng. 2007; 24:381–403. [PubMed: 17627883]

[104]. Park NJ, Wang X, Diaz A, Goos-Root DM, Bock C, Vaught JD, Sun W, Strom CM. Measurement of cetuximab and panitumumab-unbound serum EGFR extracellular domain using an assay based on slow off-rate modified aptamer (SOMAmer) reagents. PLoS One. 2013; 8:e71703. [PubMed: 23990977]

[105]. Zhou W, Huang PJ, Ding J, Liu J. Aptamer-based biosensors for biomedical diagnostics. Analyst. 2014; 139:2627–40. [PubMed: 24733714]

[106]. Schmidt KS, Borkowski S, Kurreck J, Stephens AW, Bald R, Hecht M, Friebe M, Dinkelborg L, Erdmann VA. Application of locked nucleic acids to improve aptamer *in vivo* stability and targeting function. Nucleic Acids Res. 2004; 32:5757–65. [PubMed: 15509871]

[107]. Andreola ML, Calmels C, Michel J, Toulme JJ, Litvak S. Towards the selection of phosphorothioate aptamers optimizing *in vitro* selection steps with phosphorothioate nucleotides. Eur. J. Biochem. 2000; 267:5032–40. [PubMed: 10931185]

[108]. Hoshika S, Minakawa N, Matsuda A. Synthesis and physical and physiological properties of 4'-thioRNA: application to post-modification of RNA aptamer toward NF-kappaB. Nucleic Acids Res. 2004; 32:3815–25. [PubMed: 15263062]

[109]. Bandekar A, Zhu C, Jindal R, Bruchertseifer F, Morgenstern A, Sofou S. Anti-prostate-specific membrane antigen liposomes loaded with 225Ac for potential targeted antivascular alpha-particle therapy of cancer. J. Nucl. Med. 2014; 55:107–14. [PubMed: 24337602]

[110]. Gambhir SS. Using radiolabeled DNA as an imaging agent to recognize protein targets. J. Nucl. Med. 2006; 47:557–8. [PubMed: 16595486]

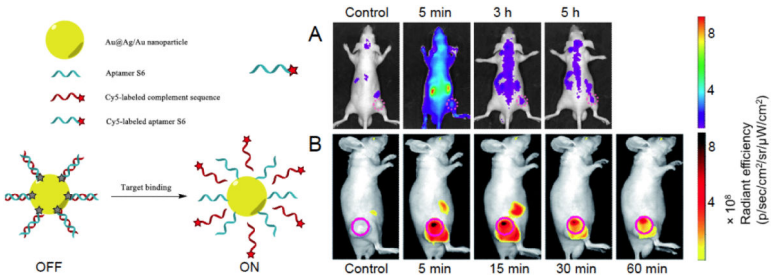

Fig. (1).

(A) Fluorescently labeled “always-on” S6 aptamer (for A549 targeting) for fluorescence imaging in A549 xenografts. Adapted with penni ssion from reference [30]. (B) The use of S6 aptamer-Au@Ag/Au nanoparticle based AAP for fluorescence imaging in A549 xenografts. Better tumor-to-background ratio was witnessed compared with directly labeled S6 aptamer. Adapted with petmission from reference [48].

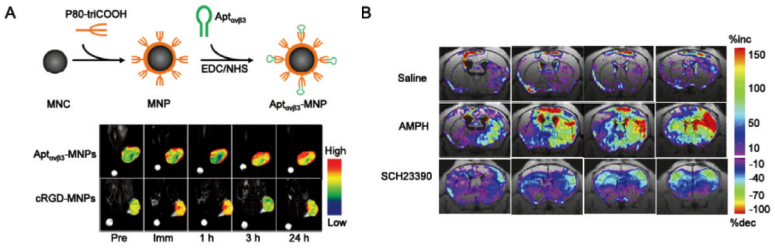

Fig. (2).

(A) An integrin $\alpha_v\beta_3$ aptamer ($Apt_{\alpha v\beta 3}$) conjugated magnetic nanoparticle (MNP) for MRI of A341 xenografts (integrin $\alpha_v\beta_3$ +). $Apt_{\alpha v\beta 3}$-MNPs showed more persistent uptake in A341 tumors compared with cRGD-MNPs (cRGD is a well-adopted targeting ligand for integrin $\alpha_v\beta_3$). Pre: preinjection; Imm: immediately following the injections; MNC: magnetic nanocrystal. Adapted with permission from reference [65]. **(B)** The $\Delta R2^*$ maps of C57B6 mice injected with 5ECdsAP1-SPIO for MRI detection of transcription factor AP1. Amphetamine (AMPH) is a strong stimulator of central nervous system which can result in the elevation of AP-1. SCH23390 is a dopaminergic receptor antagonist which can suppress the AP-1 elevation by AMPH. Saline was used as a control in this study. MRI was carried out 4 h post drug treatment and 7 h post intracerebroventricular injection of 5ECdsAP1-SPIO. Adapted with permission from reference [68].

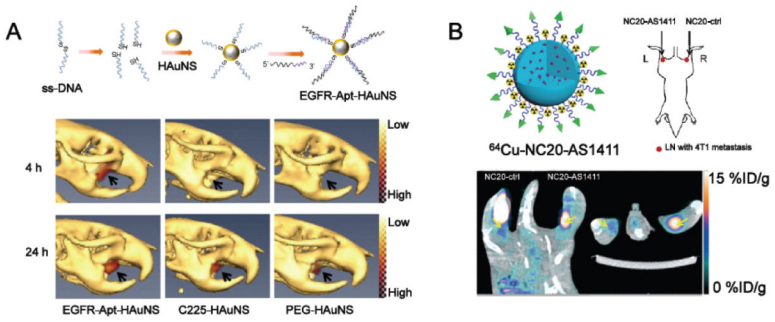

Fig. (3).

(A) The structure and application of ^{111}In-labeled, EGFR aptamer-conjugated HAuNS (EGFR-Apt-HAuNS) for SPECT/CT imaging in EGFR-positive OSC-19 xenografts. EGFR-Apt-HAuNS demonstrated faster penetration into OSC-19 tumors along with consistent accumulation when compared to EGFR-antibody (C225) conjugated HAuNS. Adapted with permission from reference [77]. **(B)** The use of ^{64}Cu-labeled, AS1411-conjugated silica nanoparticles (NC20-AS1411) for PET imaging of 4T1 tumor-drained lymph nodes. ^{64}Cu-labeled, unconjugated nanoparticles (NC20-ctrl) showed significantly lower uptake in these lymph nodes. Adapted with permission from reference [83].

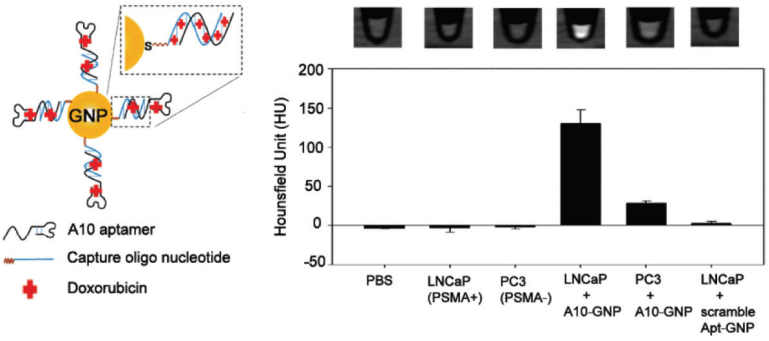

Fig. (4).

PSMA-targeting A10 aptamer conjugated GNP for cellular CT imaging. Specific recognition of PSMA-positive LNCaP cells was witnessed by a CT quantification. Adapted with permission from reference [85].

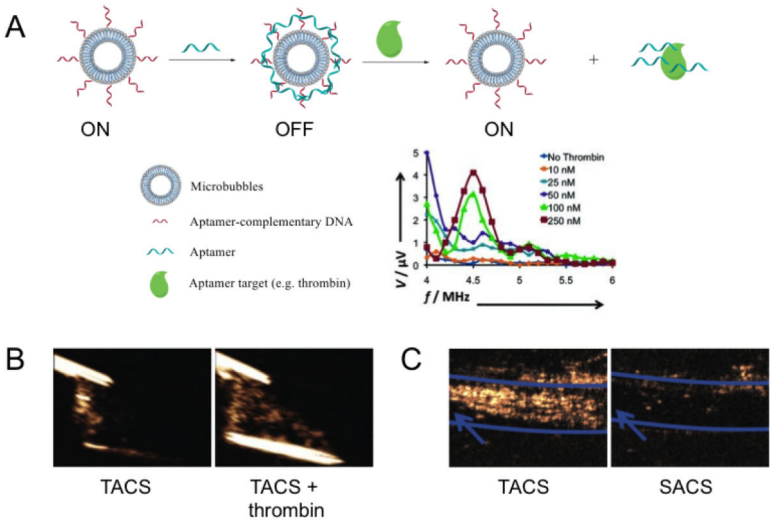

Fig. (5).

(A) The schematic illustration of producing thrombin aptamer-crosslinked sequence (TACS) conjugated microbubbles for thrombin detection. The thrombin response curve was adapted with permission from reference [93]. **(B)** *In vitro* US imaging with TACS microbubbles in active blood clots. The existence of thrombin significantly enhanced the acoustic signals from TACS microbubbles. Adapted with permission from reference [93]. **(C)** *In vivo* US imaging of deep venous thrombosis in a rabbit model. Activation of TACS microbubbles was recorded at the clot site. Scrambled-aptamer crosslinking sequence (SACS) conjugated microbubbles were used as a control to confirm the thrombin specificity of TACS microbubbles. Adapted with permission from reference [94].

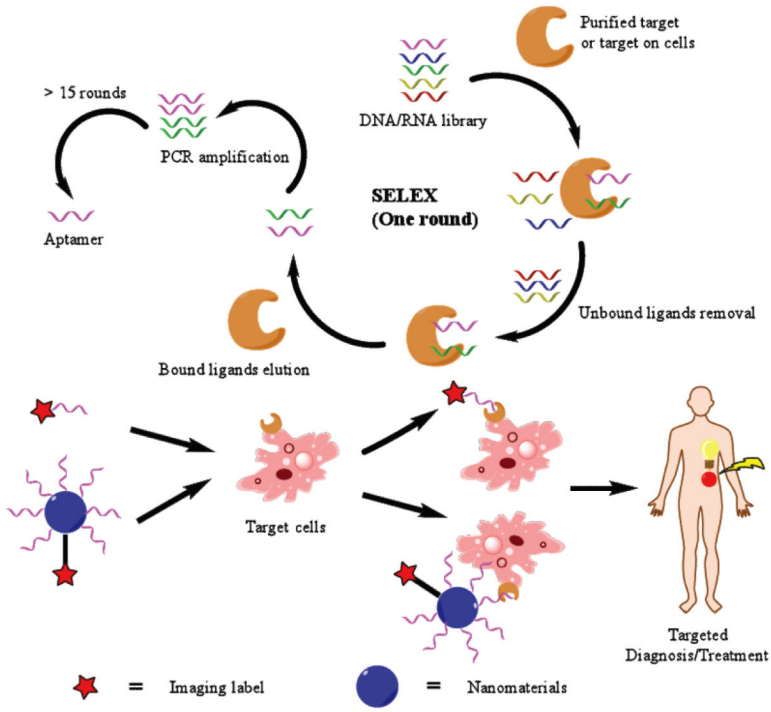

Scheme 1.

The schematic illustration of SELEX and subsequent applications of aptamer for targeted imaging.

Table 1

Representative targets for aptamer-mediated molecular imaging.

Target	Aptamer Name	Label	Imaging Modalities	K_d*	Biological Applications	Representative References
AP-1	5ECdsAPl	SPIO	MRI	N/A	Transcription monitoring	[68]
Cancer cells	TD05 (Ramos)	Cy5	Fluorescence	74.7 ± 8.7 nM	Tumor targeting	[28]
	S6	Cy5	Fluorescence	28.2 ± 5.5 nM	Tumor targeting, thermal therapy	[30, 48]
Integrin $\alpha_v\beta_3$	$Apt_{\alpha v\beta 3}$	MNP	MRI	N/A	Tumor targeting	[65]
MUC-1	MUC1 S1.3	^{99m}Tc	SPECT	0.135 nM	Tumor targeting	[75, 76]
		MPA	Fluorescence		Tumor targeting	[36]
	5TR1	SPIO	MRI	21.0 nM	Tumor targeting, drug delivery	[71]
Nucleolin	AS1411	QD	Fluorescence	< l nM	Cancer cell targeting	[33]
		^{64}Cu	PET		Tumor/metastasis targeting	[81, 83]
		Mn_3O_4@SiO_2 NP	MRI		Tumor targeting	[63]
PSMA	A10	GNPs	CT	2.1 nM	Cancer cell targeting	[85]
		QD	FRET		Cancer cell targeting, drug delivery	[54]
		SPIO	MRI		Tumor targeting	[69]
RTK-7	sgc8/sgc8c	Cy5	Fluorescence	0.80 ± 0.09 nM	Tumor targeting	[47]
		nanobubbles	US		Tumor targeting	[90]
Tenascin-C	TTA-1	^{99m}Tc	SPECT	5 nM	Tumor targeting	[74]
Thrombin	N/A	SPIO	MRI	< 5 nM	Thrombin detection	[61]
		microbubbles	US	25 nM	Deep venous thrombosis detection	[93, 94]
VEGFR-2	N/A	SPIO	MRI	0.12 nM	Vasculature targeting	[66]

* The dissociation constand (K_d) listed here is for the unconjugated aptamers. These numbers are subject to change upon the conjugation with different imaging labels or nanoplat-forms.